Land Breeze and Thermals: A Scale Threshold to Distinguish Their Effects

Yongqiang LIU*

Forestry Sciences Laboratory, USDA Forest Service, 320 Green Street, Athens, GA 30602, USA

ABSTRACT

Land breeze is a type of mesoscale circulation developed due to thermal forcing over a heterogeneous landscape. It can contribute to atmospheric dynamic and hydrologic processes through affecting heat and water fluxes on the land-atmosphere interface and generating shallow convective precipitation. If the scale of the landscape heterogeneity is smaller than a certain size, however, the resulting land breeze becomes weak and becomes mixed up with other thermal convections like thermals. This study seeks to identify a scale threshold to distinguish the effects between land breeze and thermals. Two-dimensional simulations were performed with the Regional Atmospheric Modeling System (RAMS) to simulate thermals and land breeze. Their horizontal scale features were analyzed using the wavelet transform. The thermals developed over a homogeneous landscape under dry or wet conditions have an initial scale of 2–5 km during their early stage of development. The scale jumps to 10–15 km when condensation occurs. The solution of an analytical model indicates that the reduced degree of atmospheric instability due to the release of condensation potential heat could be one of the contributing factors for the increase in scale. The land breeze, on the other hand, has a major scale identical to the size of the landscape heterogeneity throughout various stages of development. The results suggest that the effects of land breeze can be clearly distinguished from those of thermals only if the size of the landscape heterogeneity is larger than the scale threshold of about 5 km for dry atmospheric processes or about 15 km for moist ones.

Key words: land breeze, thermals, horizontal scale, large-eddy simulation, wavelet transform

1. Introduction

The landscape is often heterogeneous due to natural and anthropogenic reasons. Urbanization, deforestation, and irrigation, for example, can lead to alternating forest (wet) and bare (dry) patches. Because of the difference in land-surface energy balance between the two types of land cover, organized mesoscale circulations similar to sea breeze can be formed during daylight hours of the warm seasons, with air mass moving from the forest (wet) surface to the bare (dry) one near the ground and lifting towards the top of the planetary boundary layer (PBL) over the center of the bare (dry) surface. There has been increasing evidence for land breeze from observations (e.g., Rabin et al., 1990; Pielke and Avissar, 1990; Mahrt et al., 1994) and simulations (e.g., Segal et al., 1988; Avissar and Pielke, 1989; Pielke et al., 1992; Chen and Avissar, 1994a; Liu and Avissar, 1996; Baidya and Avissar, 2000; Weaver and Avissar, 2001; Zhao, 2002; Georgescu et al., 2003).

Land breeze can transfer sensible heat and water vapor through the PBL with magnitudes comparable to or even larger than those by turbulence (e.g., Gao et al., 1989; Mahrt and Gibson, 1992; Moeng and Sullivan, 1994). As a result, it can significantly affect regional and large-scale atmospheric processes (Baker et al., 2001; Zeng et al., 2002). Land breeze is a subgrid process in most climate models. Efforts have been made to develop parameterization schemes to include the effects of land breeze in such models. Lynn et al. (1995) and Zeng and Pielke (1995) developed parameterization schemes of heat and water transfer by land breeze using similarity theory. Liu et al. (1999), Lynne et al. (2001), and Lynne and Tao (2001) developed parameterization schemes to estimate shallow convective rainfall induced by land breeze.

The intensity of land breeze, measured by mesoscale kinetic energy (MKE), is dependent on the size of the landscape heterogeneity. For the alternating forest (wet) and bare (dry) patches, the size is the

*E-mail: yliu@fs.fed.us

distance between the centers of two adjacent patches. It was found that the land breeze is the most intense when the landscape heterogeneity has the size of the Rossby deformation ratio (about 100 km at middle latitudes) (Chen and Avissar, 1994a). When the size is smaller than a certain length, the land breeze becomes very weak and is mixed up with other thermal convections like thermals (Stull, 1988). A scale threshold of landscape heterogeneity needs to be identified to distinguish its effects on heat and water transfer from those of thermals. Avissar and Schmidt (1998) investigated the effects of surface heterogeneity on the convective boundary layer (CBL) by conducting simulations with the Regional Atmospheric Modeling System (RAMS) developed at Colorado State University (Pielke et al., 1992). Surface sensible heat flux waves with different means, amplitudes, and wavelengths were imposed as thermal forcing from an inhomogeneous land surface. It was concluded that the effects of landscape heterogeneity become insignificant when the size of the heterogeneity is smaller than about 5–10 km. Baidya et al. (2003) simulated land breeze in the Central U.S. and the Amazon using RAMS. They found a preferred length scale range of 10–20 km for land breeze.

This study seeks to determine a scale threshold of landscape heterogeneity using a different method from the one used in Avissar and Schmidt (1998). There, it was assumed that, when the scale of the landscape heterogeneity comes down to the scale of thermals, defined as the distance between two adjacent thermals, the effects of land breeze on heat and water transfer could no longer be separated from those of thermals. Therefore, the scale of thermals can be used as a length threshold for the effects of land breeze. Two related issues were also examined in this study. One was the effects of atmospheric condensation on the scale of thermals. It has been indicated in many studies that thermal convections are usually accompanied by shallow convection (e.g., Chen and Avissar, 1994b; Avissar and Liu, 1996), which would in turn affect the development of thermals. The other one was the dependence of thermals on surface moist conditions. Because of the close relation of sensible heat flux with the surface moisture content (the smaller the content, the larger the sensible heat flux), it was expected that the surface moist conditions would be a factor in the scale of thermals.

To obtain the scale threshold, two large-eddy simulations (LES) of homogeneous dry and wet landscapes were first conducted. For comparison, a third simulation of a heterogeneous landscape was conducted. The wavelet transform technique was then used to obtain scales of the simulated thermals and land breeze.

2. Methodology

2.1 *Simulation of thermals and land breeze*

The scale features of turbulent flows have been analyzed traditionally from time series of measurements near the ground surface, which gives pictures at individual locations over a long period. Remote sensing has been another useful technique to detect the spatial cross-sectional structure at separate times. LES has emerged as an advanced technique. It is capable of providing pictures of convections in both the time and space domains with high resolution and frequency (e.g., Moeng, 1984; Mason, 1994; Chen and Dudhia, 2001). LES also provides a tool to conveniently compare features of large eddies over different landscapes.

The LES model RAMS was used in this study to simulate thermals and the land breeze. The model consists of a set of non-hydrostatic, compressible dynamic equations, a thermodynamic equation, and a set of cloud micro-physical equations. There are multiple options of physical process parameterization schemes subject to different objectives of the simulations. Vertical and horizontal turbulent eddy mixing is parameterized using the 2.5-level scheme suggested by Mellor and Yamada (1982), in which the mixing coefficients are determined from a prognostic equation for turbulence kinetic energy (TKE) formulated by Yamada (1983). The radiative flux schemes in the atmospheric surface layer of Chen and Cotton (1983), the explicit cloud micro-physical scheme of Tripoli and Cotton (1982), and the soil model of Tremback and Kessler (1985) are used to compute atmospheric radiation, heat, water and momentum exchanges on the air-land interface, and cloud and precipitation processes.

A two-dimensional domain in the x (west-east) and z (vertical) directions was adopted. The horizontal length of the domain is 180 km with a resolution of 250 m (721 total horizontal grid points). There are 40 vertical levels with the top one at about 9 km. The vertical resolution is finer near the land surface and becomes progressively coarser with height. It is expected that, at such a high resolution, structures of thermals and mesoscale circulations can be identified by the model. The soil has eight layers extending down to a depth of 0.5 m.

Three simulations were performed: (1) HOMODRY, whose landscape is homogeneously dry soil with no water content at the initial time. Soil moisture itself changes with time, as calculated by the soil model in RAMS. (2) HOMOWET, which is the same as HOMODRY except for wet soil fully-irrigated at the

initial time. (3) INHOMO, whose landscape is composed of alternating dry and wet patches at the initial time. Each pair of patchs is 60 km wide (30 km for dry and 30 km for wet). The patches were assumed indefinitely long in the y-direction. For this ideal structure of patches, two-dimensional simulations can be confidently used (Avissar and Liu, 1996).

Each simulation was initialized horizontally homogeneously at 0600 local time using a sounding at about 34°N, 100°E on 28 July, 1989 [shown in Fig. 1 of Liu et al. (1999)] taken from the First ISLSCP (International Satellite Land Surface Climatology Project) Field Experiment (FIFE). Each simulation was run until 2200 local time with a time step of two seconds.

2.2 *Identification of scales*

The complexity of turbulent motions makes it difficult to easily identify the features of various scales from outputs of LES. Spectral or signal analysis techniques are needed to extract them. The wavelet transform, introduced by Morlet et al. (1982a and b) about two decades ago, was used to identify scale features of thermals and the land breeze. This technique, similar to the Fourier transform, is a tool to extract cyclic information (various spectra or scales) hidden in a series, or to represent the series with certain-degree filtering. But unlike the Fourier transform, the wavelet transform is conducted in the scale-location (space or time) domain, which enables one to identify not only various scales but the occurrence of abrupt events with a certain scale. In addition, its scale-location resolution is dependent on a scale parameter. These properties are especially useful to analyze large-eddy motions in the CBL, which are substantially non-stationary and
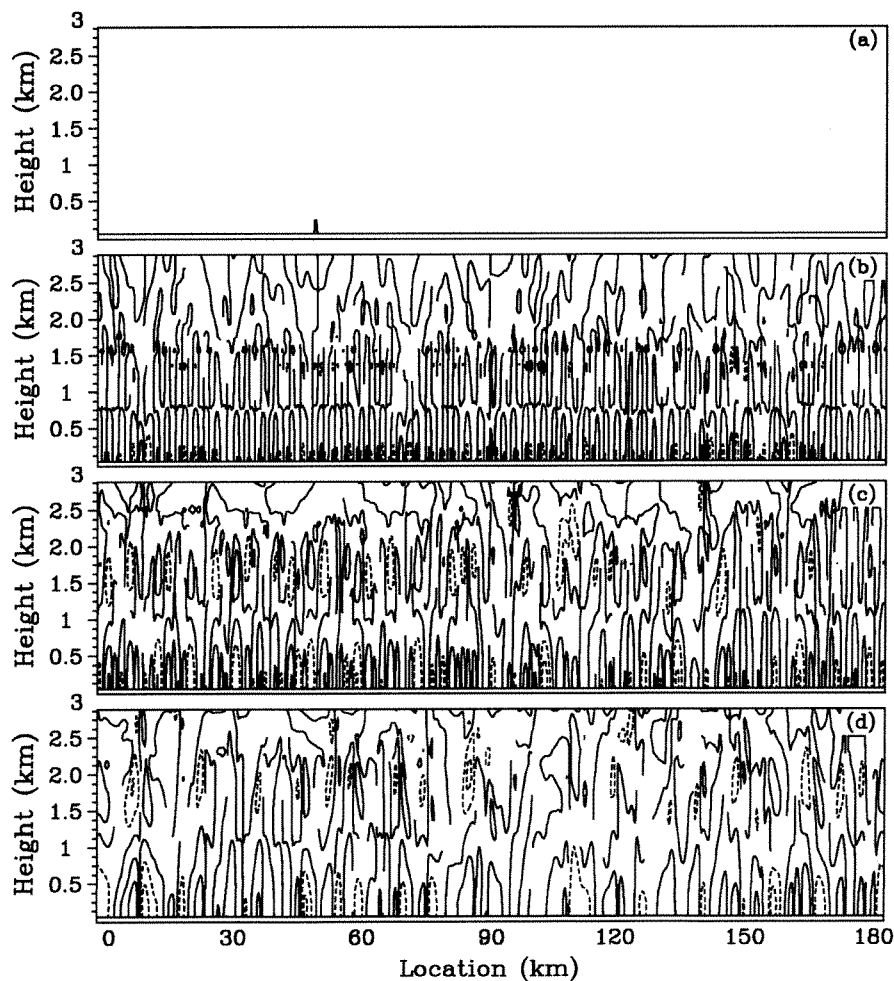

Fig. 1. Horizontal component of motions developed over a dry surface (a) 1000, (b) 1200, (c) 1400, and (d) 1600 LST. The contour interval is $2 \, \mathrm{m \, s}^{-1}$. Solid and dashed lines represent positive (westerly wind) and negative (easterly wind), respectively.
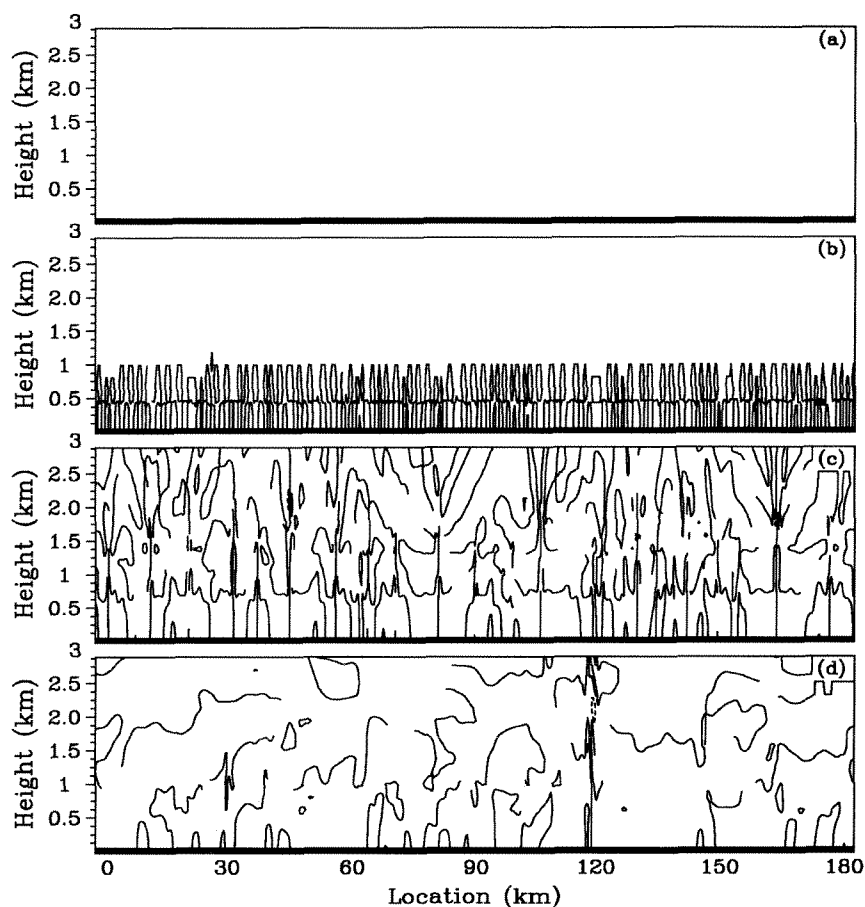
Fig. 2. Same as Fig. 1 except for a wet surface with a contour interval of 1 m s^{-1}.

nonlinear with a varied horizontal distribution, especially over heterogeneous landscapes.

Because of these unique properties, wavelet transforms have been widely used for theoretical analysis and practical application (e.g., Meyer, 1993). Guo and Li (1993) used the wavelet technique on turbulent data of temperature and vertical velocity within and above a deciduous forest and indicated that the technique clearly revealed coherent structures of atmospheric motions. Kumar and Foufoula-Georgiou (1993a and b) found some scaling properties and relationships between different scales in strong convective precipitation by using the wavelet transform. Farge (1992) and Kumar and Foufoula-Georgiou (1994) gave a comprehensive review of its application in turbulence and geophysics, respectively.

The wavelet transform of a series [say, $f(x)$] is defined as (Kumar and Foufoula-Georgiou, 1994)

$$W_f(\lambda, x) = \int_{-\infty}^{\infty} f(u)\psi_{\lambda,x}(u)du , \qquad (1)$$

$$\psi_{\lambda,x}(u) \equiv \frac{1}{\sqrt{\lambda}}\psi\left(\frac{u-x}{\lambda}\right) , \qquad (2)$$

where $\lambda(> 0)$ is a scale parameter, x a location parameter, and the function $\psi_{\lambda,x}(u)$ is wavelet with the properties of zero mean and normal distribution.

The wavelet variance, the integration of the module of the wavelet transform over entire locations, gives a measure of the relative contribution of a certain scale to total energy:

$$E(\lambda) = \int_{-\infty}^{\infty} |W_f(\lambda, x)|^2 dx . \qquad (3)$$

In the present analysis, the Morlet wavelet (Morlet et al., 1982a and b)

$$\psi(u) = \pi^{-1/4}e^{-i\omega_0 u}e^{-u^2/2} \qquad (4)$$

was adopted, where ω_o is specified with the value of 5. The Morlet wavelet has been used widely in meteorological analysis of geophysical processes (see, for example, Lau and Weng, 1995).
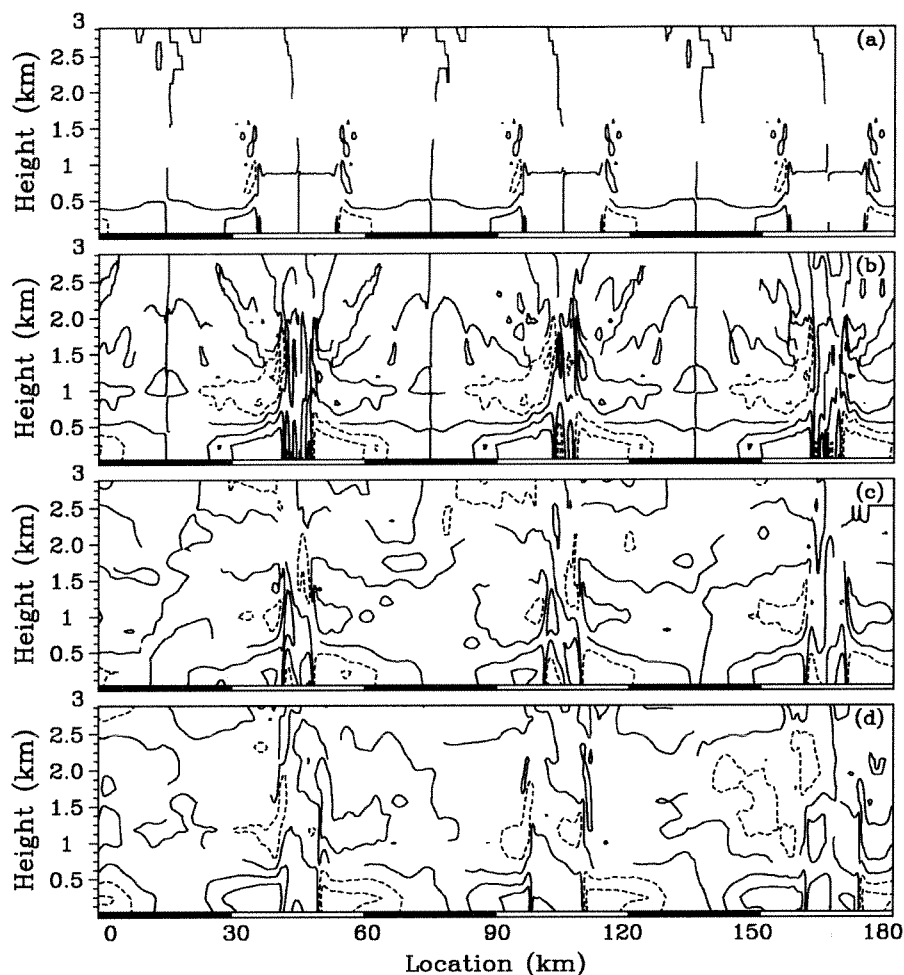
Fig. 3. Same as Fig. 1 except for a heterogeneous landscape. The filled (unfilled) horizontal bars at the bottom of the figure indicate the wet (dry) patches of the ground.

For practical application, the parameters λ and x in Eq. (1) needed to be discretized and the integration approximated by summation. The range of the summation is $x \pm m/2$, where m is an even integer and not greater than the sample size of the series. Notice that a limited sample size in a discrete series would generate an edge effect of the calculation, which means that the scale information at the two edges of the series may be unrealistic.

3. Results

3.1 *Simulated thermals and land breeze*

Figure 1 shows thermals over the dry surface at the four times of 1000, 1200, 1400, and 1600 LST (local standard time) in HOMODRY, demonstrated by the u component of velocity. The thermals start to develop at 1000, when only a weak thermal with a height of about 0.5 km can be identified at the location of about

45 km. Thermals are found over the entire domain at 1200. They reach a height of about 1.5 km. Thermals become more intense and higher at 1400. They remain almost unchanged in the next two hours, but the number of thermals is reduced. Let us look at the motion at the location of about 10 km at 1600. The u component is positive (westerly wind) on the left and negative (easterly wind) on the right below 1 km, indicating convergence of air flows. In contrast, it is negative on the left and positive on the right between 1 to 2 km, indicating divergence of air flows. The magnitude of the u component is about 3 m s^{-1}. The vertical component of velocity (not shown) indicates upward air flows, which connect the convergent air air flows near the ground with the divergent ones near the top of the CBL. This is a typical structure of a thermal in the $x - z$ domain. Thermals with the same structure are found across the horizontal domain.
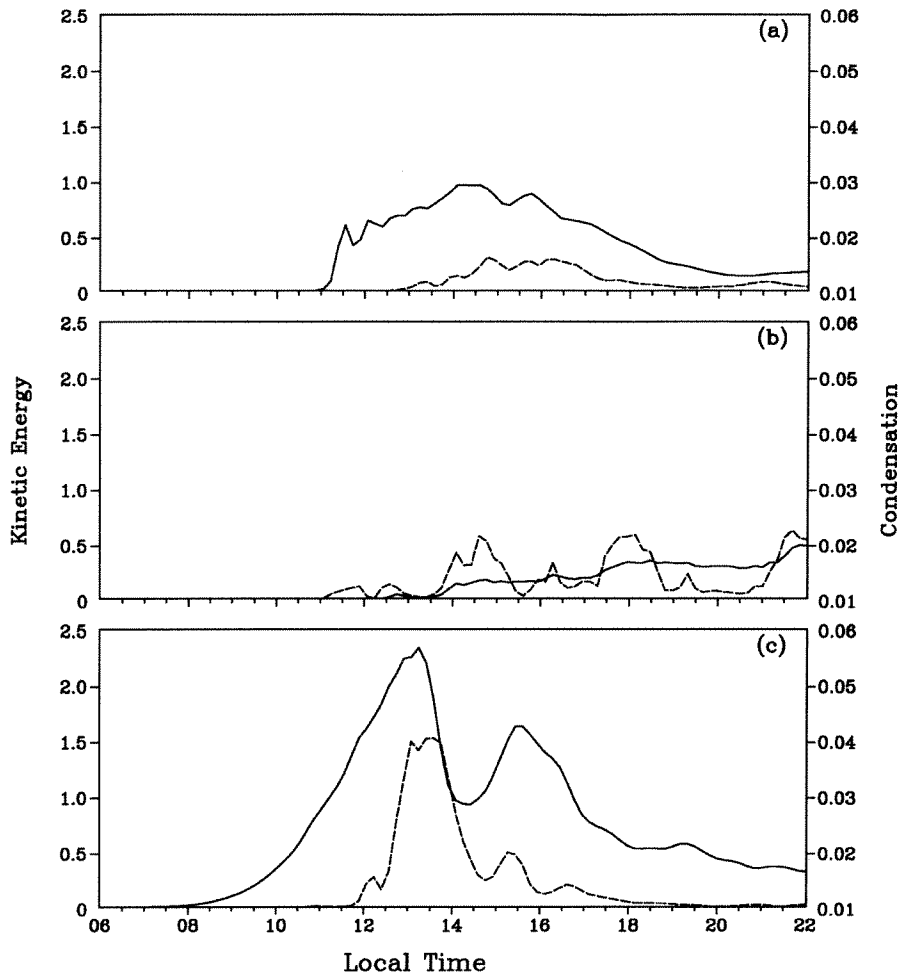
Fig. 4. Variations of mesoscale kinetic energy (kg m^2 s^{-2}) (solid lines) and cloud water mixing ratio (g kg^{-1}) (dashed lines) averaged over the $x - z$ domain. Panels (a) and (b) are for thermals over a dry and wet surface respectively, and (c) is for a land breeze over a heterogeneous surface.

Thermals over the wet surface in HOMOWET (Fig. 2) are uniformly distributed in the horizontal direction with the top reaching about 1 km at 1200. The number of thermals is significantly reduced and the height is increased to 1.5 to 2 km at 1400. Two hours later, the intensity of thermals is reduced except the one located at about 120 km.

A major feature in INHOMO is the development of a land breeze (Fig. 3). At 1000, two separate branches of circulation appear near the two ends of each dry patch. They move toward the middle of the patch and gain intensity with time. The two branches continue to move towards each other and eventually merge into a single intense convection at 1200. The circulations reach a height of about 2 km. They remain during the next four hours though the intensity is reduced.

There are two major differences between Figs. 1 and 2 at 1400 and 1600 (panels c and d) . The thermals over the dry surface are much stronger and appear in a much greater number (therefore, smaller scale) than those over the wet surface. Buoyancy and wind are two important factors in thermal development. The larger sensible heat flux from the ground should be responsible for the large intensity of the thermals over the dry surface. Over the wet surface, on the other hand, sensible heat flux is small. Meanwhile, more water transport into the atmosphere leads to condensation within thermals, which reduces instability of the lower atmosphere due to the release of latent heat. This means that the background wind, which depresses the development of thermals, becomes relatively important. As a result, many thermals disappear in the afternoon.
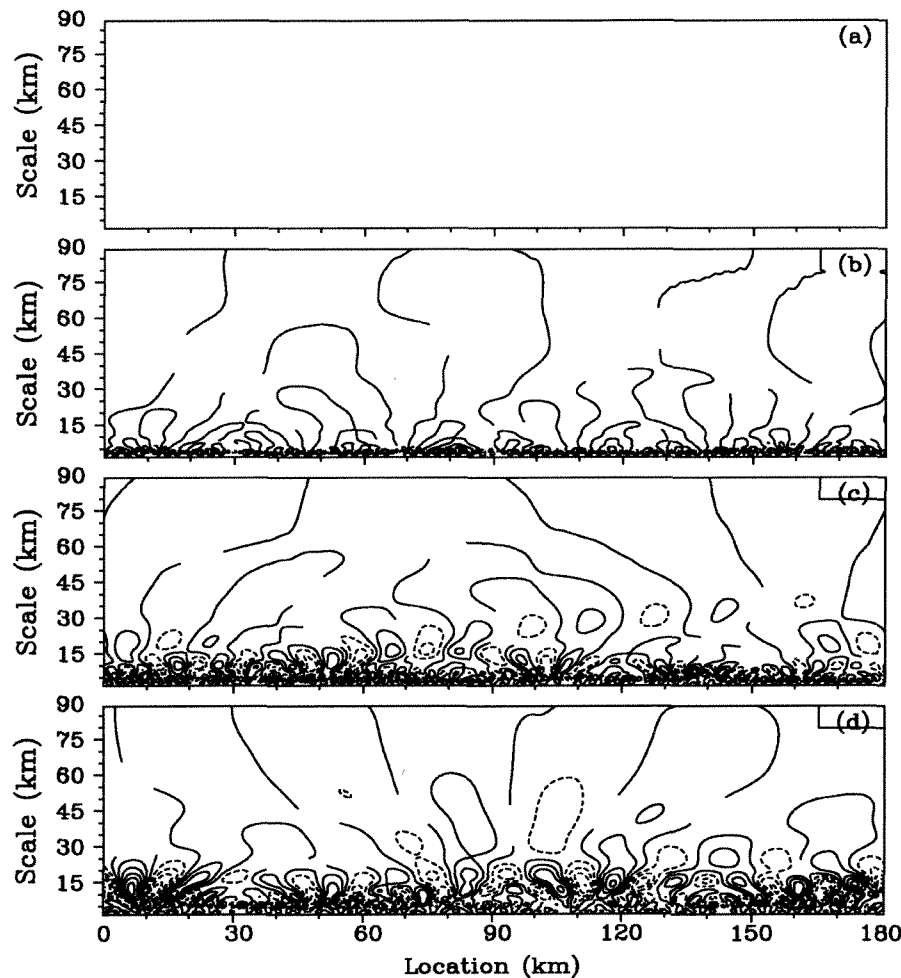
Fig. 5. Wavelet transform of the horizontal component of velocity at the height of 100 m over a dry surface. (a) 1000, (b) 1200, (c) 1400, and (d) 1600 LST. The contour interval is 2. The solid and dashed lines indicate positive and negative values, respectively.

Figure 4 shows temporal variations of the intensity of thermals and the land breeze, measured by mesoscale kinetic energy (i.e., half of the product of mass and the sum of the square mesoscale velocity components), as well as the vertically averaged cloud water mixing ratio. The intensity of thermals over the dry surface increases gradually from 1100 LST and reaches its largest value around 1400. A substantial amount of mesoscale kinetic energy remains until early evening. Condensation occurs about two hours after the initiation of thermals. Evaluation of condensation closely follows that of the intensity of thermals with a lag of about half an hour. In comparison, thermals over the wet surface are weaker. The intensity increases gradually until the end of the simulation. Condensation occurs at the time when the thermals

have just initiated and are very weak. Unlike the dry surface, condensation over the wet surface fluctuates significantly with time. Large amounts of condensation are found around 1500, 1800, and 2200. The land breeze starts to develop as early as at 0800. The intensity increases gradually until 1300. The maximum intensity is about 2.5 times that of the thermals over the dry surface. There is a second peak of mesoscale kinetic energy at about 1530. Condensation starts at about 1130 and follows that of the land breeze intensity closely. Thermals and the land breeze have very different development courses with time over various landscapes, as shown in Fig. 4. For example, when the land breeze is in the build-up phase in the morning (Fig. 4c), there is little thermal activity over the wet landscape (Fig. 4b).
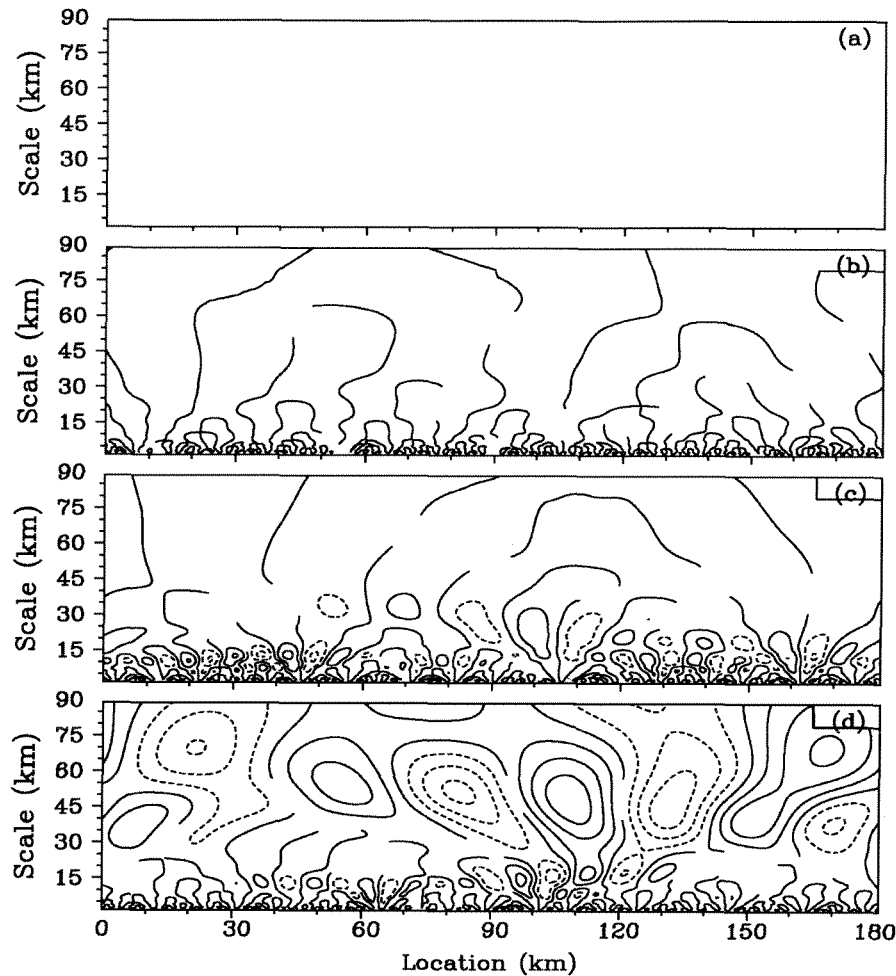
Fig. 6. Same as Fig. 5 except for a wet surface with a contour interval of 1.

3.2 *Scales*

Figure 5 shows the wavelet transform of the horizontal component of velocity, u. The wavelet transform is calculated and displayed on a scale-spaceb domain, which includes 361 grid points (90 km) in the scale direction (vertical) and 721 grid points (180 km) in the location direction (horizontal). For the wavelet transform at the grid points near the left boundary, the domain is extended leftward. A cyclic lateral boundary condition is assumed to specify u values for the extended domain. The same is done for the right boundary. The wavelet transform is conducted for the u field at the height of 100 m. The scale features are basically identical at various heights within the thermals due to strong vertical eddy mixing.

The wavelet transform pattern, such as that shown in Fig. 5 is characterized by alternative positive and negative centers oriented in both the scale and location directions. The number of individual positive (or

negative) centers in the scale direction indicates how many separate scales are involved in thermals or the land breeze. The variation in the location direction reflects the localization of these scales. For a certain scale parameter λ and location x, the wavelet transform $W_f(\lambda, x)$ is determined by W_f around x and an oscillation period related to λ. Actually, the real part of the Morlet wavelet transform is a sort of weighted smoothing average. The weight factor is a product of a cosine function, whose period is decided by λ (as well as ω_o), and an amplitude, which gradually reduces with the increase of distance from x. A positive (negative) center of $W_f(\lambda, x)$ means that the values of W at x and other locations with integral times of $2\pi\lambda/\omega_o$ in distance from x are relatively large positive (negative).

The thermals over the dry surface do not show a wavelet structure until 1200. The motions have a scale smaller than 5 km, which are distributed uniformly in the location direction at this time. This scale becomes
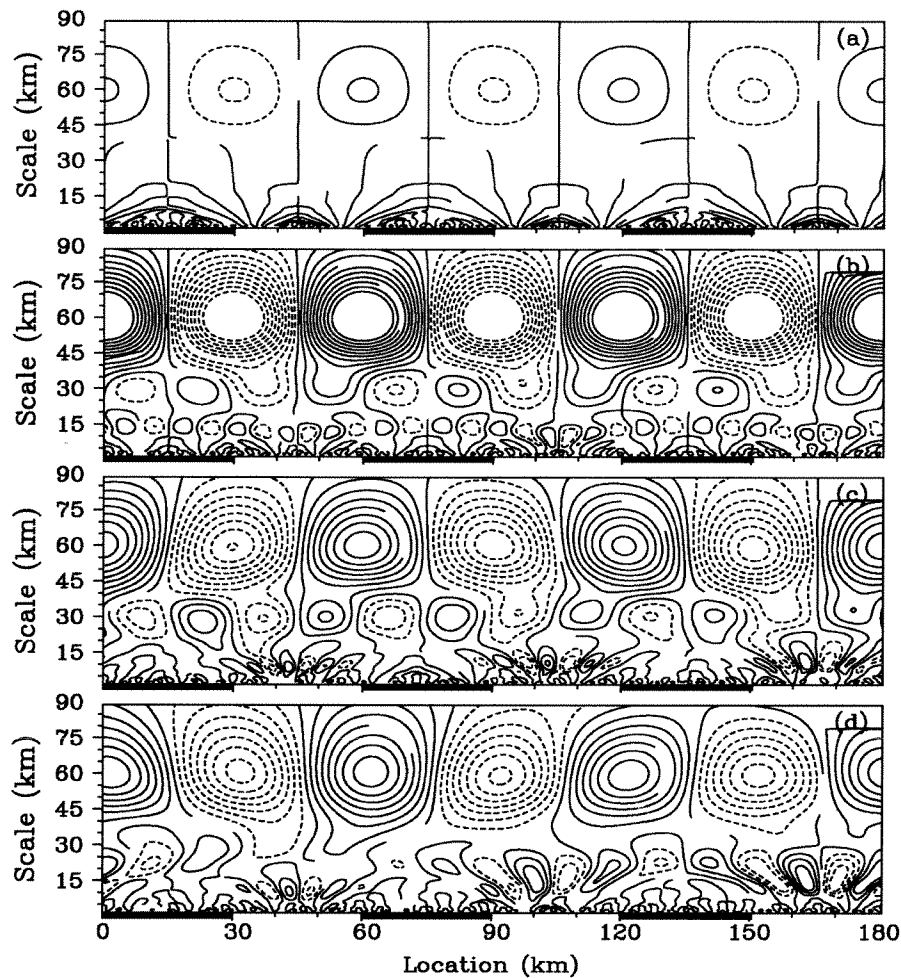
Fig. 7. Same as Fig. 5 except for the horizontal component of velocity at the height of 500 m over a heterogeneous landscape. The filled (unfilled) horizontal bars at the bottom of the figure indicate the wet (dry) patches of the ground.

more significant at 1400 and 1600. In addition, other scales from 10 to 30 km can be found, which reflects the inhomogeneous distribution of the scale in the location direction.

The thermals over the wet surface (Fig. 6) have a larger scale in the late afternoon. At 1600, there are two scales of 5 and 10 km. Another scale of 50 km or larger is found. But as seen in Figure 3, this scale is less meaningful because there is only a single thermal remaining instead of a cluster of thermals at this time.

There are three scales with motions over the heterogeneous surface (Fig. 7). One of them is 60 km, which is dominant at 1200, 1400, and 1600. This is the size of the landscape heterogeneity. A second scale is about 30 km, noticeable at 1200 and 1400, which reflects the two branches of mesoscale circulations at the two ends of each dry patch. A third scale is about 5–10 km, which is the most significant at 1000. This scale

represents the thermals within a dry or wet patch.

3.3 The effects of condensation on scales

Figure 8 depicts the temporal scale evolution of the thermals and land breeze. Over the dry landscape, the thermals have a scale of 2–3 km at about 1030. It remains mostly unchanged until 1300, when it jumps to about 8 km. The scale then increases gradually to about 14 km in the next three hours. The scale increases to about 20–25 km at 1700. Figure 4 shows that condensation occurs at about 1300, suggesting that the jump of scale at about 1300 could result from the condensation. Over the wet landscape, the thermals also have a scale of 2–3 km before it jumps to about 10 km at 1300 when a large amount of condensation occurs. The scale jumps again to about 30 km between 1400 and 1500. Over the heterogeneous surface, the scale of 60 km is dominant during most of
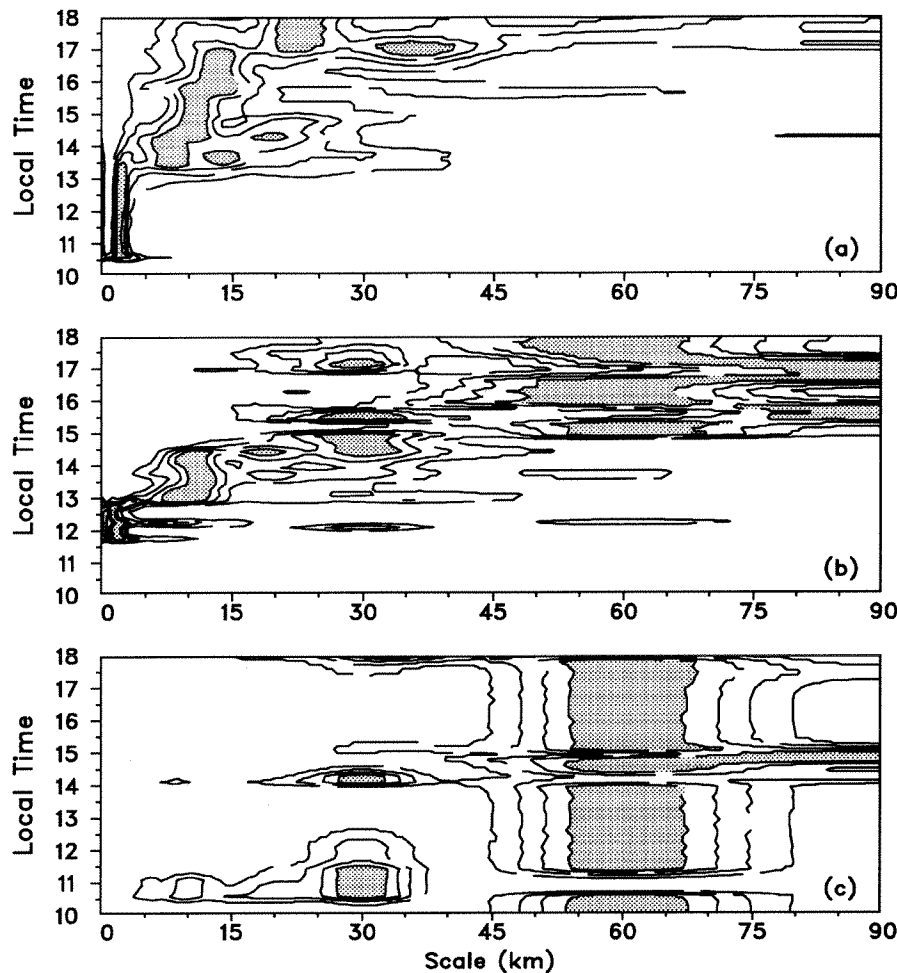
Fig. 8. Temporal variations of wavelet variance of the horizontal component of velocity at 500 m. The value of a scale at a particular time is divided by the maximum value among all scales at that time. Values greater than 0.8 are shaded. (a) dry, (b) wet, and (c) heterogeneous surfaces.

the development period of the land breeze.

Condensation of water vapor happens in the upper CBL. The potential heat released with the condensation leads to increased temperature at this level. The atmospheric instability of the CBL, originally generated due to sensible heat transfer from the surface, therefore becomes weaker. From the solution of the analytical model described in the Appendix, the scale index of a thermal convection, L_α, is inversely proportional to the degree of atmospheric instability (the absolute value of S). In other words, the scale becomes larger when the instability becomes weaker. This could be one of the possible reasons for the scale jump of the thermals occurring at about 1300 over the homogeneous dry or wet landscape.

The scale index is also dependent on two other factors. Background wind depresses the vertical expan-

sion of air mass, making it difficult for air mass to expand vertically. In addition, the scale is proportional to the height of a thermal. When a thermal gains buoyancy due to heating on the ground, it expands in both the vertical and horizontal directions, leading to the increase in thermal height and width simultaneously. Note that, because the focus of this study is on the role of the thermal forcing of the landscape, a simple background wind with a constant value in space and with time was assumed. Thus, atmospheric instability is mainly produced by the sensible heat flux rather than background wind shear.

3.4 *A length threshold for distinguishing the effects of landscape heterogeneity*

The typical scale of thermals over the homogeneous landscape changes from 2–5 to 10–15 km before and af-

ter condensation. When the pattern of multiple thermals in the horizontal direction starts to disappear in the late afternoon, the scale becomes even larger. The land breeze developed over the heterogeneous landscape, on the other hand, has a major scale identical to the size of the landscape heterogeneity throughout all stages of the development. As assumed in the introduction section, the effects of land breeze on heat and water vapor transfer cannot be clearly separated from those of thermals if the size of the landscape heterogeneity is not much larger than the scale of the thermals. Therefore, a scale of about 2–5 km can be proposed as a scale threshold to distinguish the effects of landscape heterogeneity from those of thermals for the atmosphere processes without condensation involved. This threshold is a little bit smaller than that proposed by Avissar and Schmidt (1998), who suggested a length of 5–10 km.

If condensation is involved, however, the threshold will be increased to about 15 km. This means that the effects of landscape heterogeneity should be taken into account only if the patch size is larger than 15 km. It was shown in Baidya et al. (2003) that, although the mesoscale circulations first appear at multiple scales in response to the forcing from the actual landscape heterogeneity in the Central U.S. and the Amazon, only those of circulations with a scale between 10–20 km remain for a long time. Both this result and the present study suggest that the effects of landscape heterogeneity with a size smaller than 10–20 km would be less meaningful to include in large-scale models such as general circulation models (GCMs).

4. Summary

Thermals over a homogeneous landscape and land breeze over a heterogeneous landscape have been simulated using the Regional Atmospheric Modeling System. The horizontal scale features of the model outputs have been analyzed using the wavelet transform. An analytical model has also been analyzed to examine the factors for the horizontal scale of thermals. The results indicate that:

(1) The thermals developed over a homogeneous dry or wet surface have a scale of about 2–5 km during the initial development stage.

(2) The scale jumps to about 10–15 km during the stage of major development when significant condensation occurs. The reduced degree of atmospheric instability due to the release of condensation potential heat could be one of the contributing factors for the scale increase.

(3) The land breeze developed over the heterogeneous landscape has a major scale identical to the size of the dry-wet patches throughout all stages of the development of the mesoscale circulations. There are also shorter scales representing thermals developed over the dry portion of the patches.

(4) The effects of the land breeze can be clearly distinguished from those of the thermals only if the size of the landscape heterogeneity is larger than the scale threshold of about 5 km for dry atmospheric processes or about 15 km for moist atmospheric processes.

The result (3) should be dependent on the size of the landscape heterogeneity. For a dry-wet patch size as large as 200 km, it is unlikely that a mesoscale circulation induced by the heterogeneity would develop to the size of the patch. The intensity of landscape-induced circulations becomes weaker if the landscape heterogeneity size is larger than about 100 km (Chen and Avissar, 1994a). The development process of land breeze circulation may provide an explanation. The circulation branches first develop at the dry-wet intersections in the morning hours (see Fig. 3a). They move towards the center of the dry land with time (Fig. 3b). If the patch size is too large, there would not be enough time for the two branches to merge to form a complete mesoscale circulation before they die down in the afternoon.

It should be noted that atmospheric conditions without strong background wind were considered in this research. Convections induced by landscape heterogeneity would become less significant with increased background wind (Chen and Avissar, 1994 a and b). In addition, the simulated thermals and land breeze in the two-dimensional domain would be different from those simulated in a three-dimensional one. The difference, however, is expected mainly in the magnitude rather than in the scale of thermals (Avissar and Liu, 1996).

Vertical wind shear is another important mechanism for turbulence development in addition to the thermal forcing on the ground. A constant wind has been used in the simulation from the consideration of a general condition for the generation of land breeze. Land breeze develops usually in a calm-wind atmosphere because heat exchanges with moderate or strong winds can effectively diminish the horizontal thermal contrast induced by the landscape heterogeneity. Thus, land breeze is basically a thermal issue. Many previous simulations studies (e.g., Chen and Avissar, 1994a) have used an atmospheric background with light winds and virtually no vertical wind shear. However, there might be some exceptions. One example is that, thermals or land breeze circulations are first initiated under a light background; the wind and its vertical shear increase later due to, e.g, invasion of

a synoptic system. This can substantially affect the thermals or land breeze at their later-stage development. These exception cases have yet to be examined. Thus, the results from this study are only applied to thermals and land breeze developed in calm weather.

APPENDIX

The thermal convection model and analytical solution

Assume a static and incompressible atmosphere in the $x - z$ section with constant background wind and an instable thermal stratification. Using the atmospheric equations for thermal convection (Yang et al., 1983), but neglecting horizontal turbulent heat and momentum transfer, we have:

$$u\frac{\partial u}{\partial x} + w\frac{\partial u}{\partial z} = -c_p\Theta\frac{\partial \pi}{\partial x} \, , \tag{A1}$$

$$u\frac{\partial w}{\partial x} + w\frac{\partial w}{\partial z} = -c_p\Theta\frac{\partial \pi}{\partial x} + \lambda\theta \, , \tag{A2}$$

$$u\frac{\partial \theta}{\partial x} + w\frac{\partial \theta}{\partial z} + Sw = 0 \, , \tag{A3}$$

$$\frac{\partial u}{\partial x} + \frac{\partial w}{\partial z} = 0 \, , \tag{A4}$$

where u is the horizontal component of velocity, which is composed of background U and perturbation; w is the vertical component of velocity; θ is the potential temperature perturbation; $\pi = (p/p_0)^{R/c_p}$ with p and p_0 being the pressure perturbation and the value at the sea-surface level, and R and c_p being the gas constant and specific heat at constant pressure; $\lambda = g/\Theta$; $S = \partial\Theta/\partial z < 0$ (instability stratification), where Θ is the background potential temperature. Θ in (A1) and (A2) is assumed to be constant. The boundary conditions are:

$$\theta = w = 0 \, , \text{ and } u = U \, , \text{ as } |x| \to \infty \, , \tag{A5}$$

$$w = 0 \, , \text{ at } z = 0 \, , \, H \, . \tag{A6}$$

Using the stream function, ψ:

$$u = -\frac{\partial \psi}{\partial z} \, , \tag{A7}$$

$$w = \frac{\partial \psi}{\partial x} \, , \tag{A8}$$

and the Jacobi Operator:

$$J(A, B) = \frac{\partial A}{\partial x}\frac{\partial B}{\partial z} - \frac{\partial B}{\partial x}\frac{\partial A}{\partial z} \, , \tag{A9}$$

Eq. (A3) can be written as:

$$J(\psi, \theta + Sz) = 0 \, , \tag{A10}$$

$$\theta + Sz = f_1(\psi) \, , \tag{A11}$$

where $f_1(\psi)$ is an arbitrary function of ψ. From Eq. (A7) and considering Eq. (A5):

$$z = -\frac{\psi}{U} \, , \tag{A12}$$

$$f_1(\psi) = -\frac{S}{U}\psi \, . \tag{A13}$$

Thus,

$$\theta = -\frac{S}{U}(\psi + Uz) \, . \tag{A14}$$

The vorticity equation can be derived from the momentum Eqs. (A1) and (A2):

$$u\frac{\partial \zeta}{\partial x} + w\frac{\partial \zeta}{\partial z} + \lambda\frac{\partial \theta}{\partial x} = 0 \, , \tag{A15}$$

where vorticity $\zeta = \Delta\psi$ and Δ is the Laplace operator. Applying Eqs. (A7), (A8), and (A12):

$$J\left(\psi, \Delta\psi + \frac{\lambda S}{U}z\right) = 0 \tag{A16}$$

$$\Delta\psi + \frac{\lambda S}{U}z = f_2(\psi) \, , \tag{A17}$$

where $f_2(\psi)$ is an arbitrary function of ψ:

$$f_2(\psi) = \frac{\lambda S}{U}z = -\frac{\lambda S}{U^2}\psi \, . \tag{A18}$$

Then

$$\Delta\psi + \frac{\lambda S}{U^2}\psi = 0 \, , \tag{A19}$$

where $\Psi = \psi + Uz$. The following solution for Eq. (A19) satisfying the boundary conditions can be obtained using the variable separation method:

$$\psi = -Uz + c\sum_{n=1}^{\infty}\sin(\gamma z)e^{-\alpha|x|} \tag{A20}$$

$$\theta = -\frac{S}{U}c\sum_{n=1}^{\infty}\sin(\gamma z)e^{-\alpha|x|} \, , \tag{A21}$$

where $\gamma = n\pi/H, \alpha = (\gamma^2 - \lambda S/U^2)^{1/2}$, and c is a constant. For one single thermal, $n = 1$. Integrating Eq. (A21) from $z = 0$ to $z = H$ at $x = 0$ leads to $c = -(\pi U)\bar{\theta}/(2S)$, where $\bar{\theta}$ is the vertically averaged θ at $x = 0$, which can be approximately estimated from sensible heat flux. Perturbations in velocity are:

$$u - U = \frac{\pi^2 U}{2SH}\bar{\theta}\cos\left(\frac{\pi}{H}z\right)e^{-\alpha|x|} \tag{A22}$$

$$w = \alpha\frac{\pi U}{2S}\bar{\theta}\frac{x}{|x|}\sin\left(\frac{\pi}{H}z\right)e^{-\alpha|x|} \, . \tag{A23}$$

They represent a circulation in the $x - z$ section with airflows from left to right near the surface, upwards over the area of $x > 0$, from right to left near the top of the CBL, and downwards over the area of $x < 0$. The perturbation is the strongest at $x = 0$, with discontinuity in the vertical component. The parameter α is the decay rate of the motion, and its reciprocal is the e-folding scale, which indicates a location of x where the intensity of the perturbation is reduced to e^{-1} of the perturbation at $x = 0$. This parameter therefore measures how fast the perturbation decay is with x. We use $L_\alpha = 1/\alpha$ as a horizontal scale index for thermal convection.

REFERENCES

Avissar, R., and R. A. Pielke, 1989: A parameterization of heterogeneous land-surface for atmospheric numerical models and its impact on regional meteorology. *Mon. Wea. Rev.*, **117**, 2113–2136.

Avissar, R., and F. Chen, 1993: Development and analysis of prognostic equations for mesoscale kinetic energy and mesoscale (subgrid scale) fluxes for large-scale atmospheric models. *J. Atmos. Sci.*, **50**, 3751–3774.

Avissar, R., and Y. Q. Liu, 1996: A three-dimensional numerical study of shallow convective clouds and precipitation induced by land-surface forcing. *J. Geophys. Res.*, **101**(D3), 7499–7518.

Avissar, R., and T. Schmidt, 1998: An evaluation of the scale at which ground-surface heat flux patchiness affects the convective boundary layer using a Large-Eddy Simulation model. *J. Atmos. Sci.*, **55**(16), 2666–2689.

Roy, S. B., and R. Avissar, 2000: Scales of response of the convective boundary layer to land-surface heterogeneity. *Geophys. Res. Lett.*, **27**, 533–536.

Roy, S. B., C. P. Weaver, D. Nolan, and R. Avissar, 2003: A preferred scale for landscape forced mesoscale circulations? *J. Geophys. Res.*, **108**, 8808, doi:10.1029/2002JD003097.

Baker, R. D., B. H. Lynn, A. Boone, W. -K. Tao, and J. Simpson, 2001: The influence of soil moisture, coastline curvature, and land-breeze circulations on sea-breeze initiated precipitation. *J. Hydrol.*, **2**(2), 193–211.

Chen, C., and W. R. Cotton, 1983: A one-dimensional simulation of the stratocumulus-capped mixed layer. *Bound.-Layer Meteor.*, **25**, 289–321.

Chen, F., and R. Avissar, 1994a: Impact of land-surface wetness heterogeneity on mesoscale heat fluxes. *J. Appl. Meteor.*, **33**, 1323–1340.

Chen, F., and R. Avissar, 1994b: Impact of land-surface moisture variability on local shallow convective cumulus and precipitation in large-scale models. *J. Appl. Meteor.*, **33**, 1382–1401.

Chen, F., and J. Dudhia, 2001: Coupling an advanced land-surface/hydrology model with the Penn State/NCAR MM5 modeling system. Part I: Model implementation and sensitivity. *Mon. Wea. Rev.*, **129**, 569–585.

Farge, M., 1992: Wavelet transforms and their applications to turbulence. *Annual Reviews of Fluid Mechanism*, **24**, 395–457.

Gao, W., and B. L. Li, 1993: Wavelet analysis of coherent structures at the atmosphere-forest interface. *J. Appl. Meteor.*, **32**, 1717–1725.

Gao, W., R. H. Shaw, and K. T. Paw U, 1989: Observation of organized structures in turbulent flow within and above a forest canopy. *Bound.-Layer Meteor.*, **47**, 349–377.

Georgescu, M., C.P. Weaver, R. Avissar, R.L. Walko, and G. Miguez-Macho, 2003: Sensitivity of model-simulated summertime precipitation over the Mississippi River basin to the spatial distribution of initial soil moisture. *J. Geophys. Res.*, **108**, 8855, doi:10.1029/2002JD003107.

Kumar, P., and E. Foufoula-Georgiou, 1993a: A multicomponent decomposition of spatial rainfall fields, 1. Segregation of large- and small-scale features using wavelet transforms. *Water Resour. Res.*, **118**, 2515–2532.

Kumar, P., and E. Foufoula-Georgiou, 1993b: A multicomponent decomposition of spatial rainfall fields, 2. Self-similarity in fluctuations. *Water Resour. Res.*, **118**, 2533–2544.

Kumar, P., and E. Foufoula-Georgiou, 1994: Wavelet analysis in geophysics: An introduction. *Wavelet in Geophysics*, E. Foufoula-Georgiou and P. Kumar, Eds., Academic Press Inc., 1–43.

Lau, K.-M., and H. Weng, 1995: Climate signal detection using wavelet transform: How to make a time series sing. *Bull. Amer. Meteor. Soc.*, **79**, 2391–2402.

Liu, Y. Q., and R. Avissar, 1996: Sensitivity of a shallow convective precipitation induced by land-surface heterogeneity to dynamical and cloud microphysical parameters. *J. Geophys. Res.*, **101**(D3), 7477–7497.

Liu, Y. Q., C. P. Weaver, and R. Avissar, 1999: A parameterization of shallow convection induced by landscape heterogeneity for use in GCMs. *J. Geophys. Res.*, **104**(D16), 19515–19534.

Lynn, B. H., and W.-K. Tao, 2001: A parameterization for the triggering of landscape generated moist convection, Part II: Zero order and first order closure. *J. Atmos. Sci.*, **58**(6), 593–607.

Lynn, B. H., F. Abramopoulos, and R. Avissar, 1995: Using similarity theory to parameterize mesoscale heat fluxes generated by subgrid-scale landscape discontinuities in GCMs. *J. Climate*, **8**, 932–951.

Lynn, B. H., W.-K. Tao, and F. Abramopoulos, 2001: A parameterization for the triggering of landscape generated moist convection, Part I: Analyses of high resolution model Result. *J. Atmos. Sci.*, **58**, 575–592.

Mahrt, L., and W. Gibson, 1992: Flux decomposition into coherent structures. *Bound.-Layer Meteor.*, **60**, 143–168.

Mahrt, L., J. Sun, D. Vickers, J. I. MacPherson, J. R. Pederson, and R. Desjardins, 1994: Observations of fluxes and inland breezes over a heterogeneous surface. *J. Atmos. Sci.*, **51**, 2484–2499.

Mason, P. J., 1994: Large-eddy simulation: A critical review of the technique. *Quart. J. Roy. Meteor. Soc.*, **120**, 1–26.

Mellor, G. L., and T. Yamada, 1982: Development of a turbulence closure model for geophysical fluid problems. *Rev. Geophys. Space Phys.*, **20**, 851–875.

Meyer, Y., 1993: *Wavelets: Algorithms and Applications*, SIAM, Philadelphia, 133pp.

Moeng, C.-H, 1984: A large-eddy simulation model for the study of planetary boundary-layer turbulence. *J. Atmos. Sci.*, **41**, 2052–2062.

Moeng, C.-H, and P. P., Sullivan, 1994: A comparison of shear and buoyancy driven planetary boundary flows. *J. Atmos. Sci.*, **51**, 999–1022.

Morlet, J., G. Arens, E. Fourgeau, and D. Griad, 1982a: Wave propagation and sampling theory. part 1: Complex signal and scattering in multilayered media. *Geophysics*, **47**, 203–221.

Morlet, J., G. Arens, E. Fourgeau, and D. Griad, 1982b: Wave propagation and sampling theory. Part 2: Sampling theory and complex waves. *Geophysics*, **47**, 222–236.

Pielke, R. A. and R. Avissar, 1990: Influence of landscape structure on local and regional climate. *Landscape Ecology*, **4**, 133–155.

Pielke, R. A., and Coauthors, 1992: A comprehensive meteorological model system-RAMS. *Meteorology and Atmospheric Physics*, **49**, 69–91.

Rabin, R. M., S. Stadler, P. J. Wetzel, D. J. Stensrud, and M. Gregory, 1990: Observed effects of landscape variability on convective clouds. *Bull. Amer. Meteor. Soc.*, **71**, 272–280.

Segal, M., R. Avissar, M. McCumber, and R. A. Pielke, 1988: Evaluation of vegetation effects on the generation and modification of mesoscale circulations. *J. Atmos. Sci.*, **45**, 2268–2292.

Stull, R. B., 1988: *An Introduction to Boundary Layer Meteorology.* Kluwer Academic Publishers, 666pp.

Tremback, C. J., and R. Kessler, 1985: A surface temperature and moisture parameterization for use in mesoscale numerical models. Seventh Conf. on Numerical Weather Prediction, Montreal, Canada, Amer. Meteor. Soc., 355–358.

Tripoli, G. J., and Cotton, W. R., 1982: The Colorado State University three-dimensional cloud/mesoscale model −1982. Part I: General theoretical framework and sensitivity experiments. *Journal de Recherches Atmospheriques*, **16**, 185–220.

Weaver, C. P. and R. Avissar, 2001: Atmospheric disturbances caused by human modification of the landscape. *Bull. Amer. Meter. Soc.*, *82*, 269–281.

Yang, D. S., Y. B. Liu, and S. G. Liu, 1983: *Dynamic Meteorology.* China Meteorological Press. 423pp.

Yamada, T., 1983: Simulations of nocturnal drainage flows by a q^2-l turbulence closure model, *J. Atmos. Sci.*, **40**, 91–106.

Zeng, X. B., and R. A. Pielke, 1995: Landscape-induced atmospheric flow and its parameterization in large-scale numerical models. *J. Climate*, **8**, 1156–1177.

Zeng, X. M., M. Zhao, B. K. Su, J. P. Tang, Y. Q. Zheng, Y. J. Zhang, and J. Chen, 2002: The effects of land-surface heterogeneities on regional climate: A sensitivity study. *Meteorology and Atmosphic Physics*, **81**, 67–84.